THE EFFECT OF A SPANWISE BLOWING JET ON THE SEPARATION BUBBLE LENGTH BEHIND A REARWARD FACING STEP

Thesis by

Gavien N. Miyata

In Partial Fulfillment of the Requirements

For the Degree of

Aeronautical Engineer

California Institute of Technology

Pasadena, California

1972

(Submitted May 26, 1972)

ACKNOWLEDGEMENTS

The author wishes to thank Dr. Gordon Harris for his suggestions and guidance throughout the research. Dr. Harris not only initiated the original problem but also suggested an approach to the solution. In addition the author wishes to thank Dr. H. J. Stewart and Dr. Frank Marble for their constructive criticism during the final phases of the research. Special thanks go to Mrs. Elizabeth Fox, who typed this manuscript; Mrs. Betty Wood, who drew the figures contained herein; and Mrs. Jewel Colbert, who worked to reproduce this thesis in final form. The author is also indebted to the California Institute of Technology for giving him financial support during the period of research.

Finally, the author wishes to dedicate this work to his fiancée, Ann Gibson, who showed great understanding and encouragement during the most difficult times.

ABSTRACT

The problem of the effect of a spanwise blowing jet on the flow past a rearward facing step is considered both theoretically and experimentally. The primary flow is considered to be a finite two-dimensional jet blowing past a step and the spanwise jet is assumed to blow perpendicular to this primary flow. The equations predicting the separation bubble length are derived by assuming that the two-dimensional jet is thin enough so that its radius of curvature can be determined by the pressure difference across the primary jet and the jet momentum. Then by doing a momentum balance at the reattachment point, the angle of reattachment is determined and the bubble geometry is fixed. The effect of the spanwise blowing jet is modeled by a two-dimensional sink with the sink strength given by the mass entrainment per unit length of a round jet in a semi-confined space.

The experimental work, which measured the bubble length as a function of the two-dimensional jet thickness and the strength of the spanwise blowing jet, is matched with the theoretical predictions giving the spreading parameters of the shear layers on both sides of the primary jet.

TABLE OF CONTENTS

I. Introduction

The problem of boundary layer control has been of interest in aeronautics for quite some time. Various methods have been proposed of which the three major types are suction of the low energy fluid from the boundary layer, motion of the solid wall to prevent the formation of a boundary layer, and blowing in the same direction as the outer flow in order to energize the fluid in the boundary layer. By preventing separation these methods of control help to reduce drag and stall and are therefore instrumental in the workings of high lift devices.

In 1964, Lockheed Aircraft in Georgia began conducting tests on a different approach to boundary layer control.[1] It was observed that a jet blowing spanwise over a lifting surface helped to increase the lift even past angles of attack greater than the stall angle because the spanwise blowing jet caused the flow to reattach onto the lifting surface after its initial leading edge separation. It appears that the mechanism controlling this phenomenon is due primarily to the spanwise jet entrainment. In effect, the jet is used to remove the low energy fluid from the stalled, recirculating region thereby shrinking the separation bubble.

It is the purpose of this present investigation to examine the phenomenon under somewhat idealized conditions both theoretically and experimentally. For this purpose the problem has been simplified somewhat by considering the separation bubble formed by a finite two-dimensional jet blowing past a rearward facing step and considering the bubble length as a function of the strength of another

jet placed at the base of the step, blowing perpendicular to the primary flow. Figure 1 shows a schematic of this configuration. In formulating the theory, the assumption is made that the jet profile remains unchanged by the jet curvature and thus changes only as a function of its distance, as measured along an arc, from the jet slot. By assuming that the cavity pressure in the separation bubble is constant, the two-dimensional jet centerline should be an arc of a circle within the framework of a thin jet approximation. One can then find the reattaching streamline, that is, the streamline which separates the returning flow from the main flow, with respect to this jet centerline if a streamline of the jet profile is known. If one can determine the position of the reattaching streamline at one upstream location, then he should be able to determine the position of this streamline at any other downstream location since the mass flow between the reattaching streamline and the other known streamline of the jet profile must be constant. Now the bubble length can be determined if the angle with which the jet centerline crosses the ground plane can be found. This angle is determined by forming a momentum balance near the reattachment point, and this completes the solution of determining the bubble length as a function of the two-dimensional jet thickness. Adding in the effect of the corner spanwise blowing jet, we find that the problem is only slightly modified. The spanwise blowing jet is approximated by a sink whose strength is taken to be the jet entrainment per unit length. Since the sink is constantly being fed by the outer flow, the volume flow between the top of the corner of the step and the

reattaching streamline must equal the sink flow. This fact defines the reattaching streamline as a function of the mass entrainment of the spanwise blowing jet.

The first part of the problem dealing with the calculation of the bubble length as a function of the jet thickness and step height without the action of the spanwise blowing jet was originally formulated by R. A. Sawyer.[2, 3] His solution assumed that fully developed jet similarity profiles were formed before the jet impinged onto the ground plane and thus this theory is applicable only to thin two-dimensional jets with jet thicknesses much less than the step height. The present solution continues Sawyer's solution to include thick jets, several times the step height. This approach uses shear layer profiles with a potential core as representative of the velocity profiles issuing from the two-dimensional slot. In this way the solution is applicable to jet thicknesses many times the step height although it is not applicable to the problem of infinite jet thicknesses since the momentum balance at reattachment tends to give a zero angle thereby leading to an infinite bubble length in the limit. In addition, a "semi-thin jet" approximation, which assumes that the pressure gradient across the jet can be modeled by a pressure difference divided by the jet thickness, is no longer applicable for very large jets since one reaches ambient pressures inside the jet when the jet thickness is very large.

II. Theoretical Analysis

The primary objective of this work is to create a model which will demonstrate the effect of the spanwise blowing on the length of the separation bubble behind a rearward facing step. However, before considering the total problem, we should first see if we can properly model the phenomenon of the separation bubble length as a function of the two-dimensional jet thickness. Once this part is completed, it should be a relatively simple matter to add in the effect of the spanwise blowing jet.

A. Separation Flow Model Without Spanwise Blowing Jet

The solution of this initial problem requires the determination of the reattaching streamline location, the angle of reattachment, and the geometrical formulas relating the jet thickness to the reattachment length. However, since the first two pieces of the solution require some knowledge of the jet profile, it is imperative that we establish the form we will use.

1. Two-Dimensional Jet Profile Approximation

Throughout the analysis the approximation is made that the streamwise two-dimensional jet profile is made up of a potential case of uniform velocity bounded by two shear layers, each of which has a different spreading rate in the general case. Various authors have determined that the shear layer profile can be approximated by the error integral,[4] but this analysis will instead use a hyperbolic secant to model the shear layer. This is done because the resulting form of the velocity expression is more amenable to mathematical manipulation in closed form than is the error function.

If the shear layer profile is given as a function of $\xi = \frac{\sigma y}{x}$ where σ is the spreading parameter, then the profile may be approximated by

$$\frac{u}{U} \cong \text{SECH}^2(a\xi + b) \qquad \text{where} \quad a = 0.755, \quad b = -0.899 \; .$$

The points of matching are taken to be at $\xi = 1.19$ where $a\xi+b = 0$ and at $\xi = -0.135$ where $a\xi+b = -1$. As shown in figure 2, the match between the shear layer profile as given experimentally by Liepmann and Laufer[5] and the approximation given above is quite good.

Referring to figure 3, the shear layer can be divided into two parts by the horizontal line passing through the virtual origin. The upper portion which meets the potential core is defined as δ_1 and the lower portion as δ_2. According to Liepmann and Laufer,[5] this horizontal line which passes through the origin intersects the shear layer profile at $u/U = 0.6875$ or $\xi = 0.36$. Since δ_1 and δ_2 are measured with respect to this line, it is convenient to define a new parameter, ξ', such that $\xi' = 0$ at $u/U = 0.6875$ or

$$\xi' = \xi - 0.36 \; .$$

In this way we can define the shear layer growth as a function of x.

$$\delta_1 = \frac{0.83}{\sigma} x$$

$$\delta_2 = \frac{2.36}{\sigma} x$$

Referring to figure 3, one can see that the upper profile may in general have a different spreading rate from the shear layer at the bottom part of the jet.

$$\delta_{1u} = \frac{0.83}{\sigma_1} x$$

$$\delta_{2u} = \frac{2.36}{\sigma_1} x$$

According to Prandtl's mixing length theory, we would expect the spreading of the lower shear layer to be suppressed by the wall while the spreading of the upper shear layer should be enhanced by the jet curvature. Defining ν as the ratio of the spreading parameters,

$$\nu = \frac{\sigma_1}{\sigma} \quad ,$$

we should expect $\nu \leq 1$.

In general there exists a boundary layer at the edge of the step at $x = x_o$ as shown in figure 4, and we shall attempt to approximate it by part of a shear layer. In reality there exists a non-similar transition region between the boundary layer profile at $x = x_o$ to the similarity shear layer profile farther downstream. However, for the sake of simplicity, we can assume that the boundary layer may be represented by the shear layer truncated at $\xi = -0.73$. This cutoff point was originally chosen by Sawyer[3] who matched the volume in a truncated shear layer profile with that of a boundary layer. If the boundary layer thickness at $x = x_o$ is δ_o, then

$$\delta_o = \delta_{1o} + \delta_{2o} = \frac{0.83}{\sigma} x_o + \frac{1.09}{\sigma} x_o$$

or $$\delta_o = \frac{1.92}{\sigma} x_o \quad .$$

Now that the two-dimensional jet profile, which will be used, has been defined, it is possible to calculate the jet momentum:

$$J = \rho \int_{-\infty}^{\infty} u^2 \, dy = 2\rho U^2 \frac{X}{\sigma} \alpha(x)$$

where $\alpha(x) = \frac{\sigma t}{X} + \left(0.053 - 1.09 \frac{X_0}{X}\right)\gamma$ and $\gamma = \frac{1}{2}\left(1 + \frac{1}{\nu}\right)$.

2. Position of Reattaching Streamline

Knowing the jet momentum and the two-dimensional jet profile, we can now calculate the position of the reattaching streamline. The assumption has been made that the pressure in the separation bubble is approximately constant and thus the centerline of the jet may be represented by an arc of a circle except near the reattachment point. Using the Navier-Stokes equation in cylindrical coordinates with only the lowest order terms retained,

$$\frac{\partial P}{\partial r} = \frac{\rho u_\theta^2}{r},$$

we can express the radius of curvature of the jet centerline as a function of the jet momentum and the pressure difference across the jet:

$$\Delta P = P_\infty - P_c = \frac{J}{R},$$

where P_c is the cavity pressure and P_∞ is the local ambient pressure.

Thus if we know the position of the reattaching streamline, i.e., the streamline leaving from the edge of the step, with respect to the jet centerline, we can find the bubble length if we know the angle with which the streamline intersects the ground plane. This

reattaching streamline is found by matching the volume flow between a known streamline of the shear flow ($\xi = 0.125$) and the step corner ($\xi = -0.73$) at $x = x_o$ with the volume flow at an arbitrary x between $\xi = 0.125$ and $\xi = \xi_R$. Since there is no flow through streamlines, the volume flow between $\xi = .125$ and ξ_R should be constant and this should define the reattaching streamline.

The initial volume flow at $x = x_o$ between $\xi = .125$ and $\xi = -0.73$ is

$$Q_{x_o} = \int_{\xi = -0.73}^{\xi = 0.125} u \, dy = 0.23 \frac{U_o x_o}{a\sigma} = 0.305 \frac{U_o x_o}{\sigma}$$

where $U_o = U(x = x_o)$.

Calculating the volume flow between $\xi = 0.125$ and $\xi = \xi_R$ at an arbitrary x, we find

$$Q_x = \int_{\xi = \xi_R}^{\xi = 0.125} u \, dy = \frac{Ux}{a\sigma}(-0.666 - T)$$

where

$$T = \text{TANH}(a\xi_R + b) .$$

Equating the two values for the volume flow, we arrive at an expression for T. However, this expression involves U_o/U which can be rewritten in terms of the momentum parameter $\alpha(x)$ since we know that the jet momentum, J, is constant for a two-dimensional jet. Thus we find

$$T = \text{TANH}(a\xi_R + b) = -0.23\sqrt{\frac{x_o \alpha(x)}{x \alpha(x_o)}} - 0.666$$

in terms of three parameters: $\alpha(x)$, $\alpha(x_o)$ and x_o/x.

But $\alpha(x_o)$ can be written in terms of the initial boundary layer thickness:

$$\alpha(x_o) = 1.92\left(\frac{h}{\delta_o}\right)\left(\frac{t}{h}\right) - 1.037\gamma \quad \text{for } \frac{\delta_o}{h} \text{ constant}$$

$$\text{or} \quad \alpha(x_o) = 1.92\,\frac{t}{\delta_o} - 1.037\gamma \quad \text{for } \frac{\delta_o}{t} \text{ constant}.$$

Also, x_o/x can be expressed as

$$\frac{x_o}{x} = \frac{\alpha(x) - 0.053\gamma}{\alpha(x_o) - 0.053\gamma}$$

by combining expressions for $\alpha(x)$ and $\alpha(x_o)$. Since $\alpha(x_o)$ is known as a function of h/t or δ_o/t, x_o/x can be specified in terms of $\alpha(x)$ and h/t. Thus T can be found once $\alpha(x)$ and h/t are known, so all we need now is a relationship between $\alpha(x)$ and h/t. This expression will come later in this paper.

Knowing T, we can easily find ξ'_R by inverting the expression for T. However, the particular form cannot be easily used in a computer computation since it involves the inverse hyperbolic tangent. To alleviate this difficulty, we will use an approximation adopted by Sawyer[3] in his analysis. Since the volume flow between $\xi = 0.125$ and $\xi = \xi_R$ is constant and the shear layer spreads as it goes downstream, we would expect ξ_R to be between $\xi = 0.125$ and $\xi = -0.73$. Within this region the shear layer profile may be approximated by a linear expression

$$\frac{u}{U} = \frac{1}{2}\left(1 + \frac{\xi}{2}\right) \quad .$$

Using this expression, we find

$$\xi_R' = \sqrt{1.266 - 1.22\sqrt{\frac{\alpha(x)\,X_o}{\alpha(x_o)\,X}}} - 1.36$$

and this gives us the reattaching streamline position with respect to the jet centerline.

3. Force Balance at Reattachment Point

Now if we can specify the angle with which the jet centerline meets the ground plane, we will have determined the global characteristics of the flow field, and we should therefore be able to find the separation bubble length. This impingement angle is calculated by doing a force balance on a control volume situated at the reattachment point as shown in figure 5. The mass contained in that portion of the shear layer below the reattaching streamline is constantly fed back into the separation cavity and the velocity profiles will be assumed to remain self-similar as they exit from the control volume. Thus the distance $x = x_1$ and the angle θ are defined by the fact that the distance from the edge of the shear layer to the reattaching streamline, $\bar{a}$, is equal to the vertical distance from the ground plane to the edge of the shear layer, $\bar{b}$.

Defining J_3 as the momentum at x_1 above the reattaching streamline, and J_2 as the momentum at x_1 below the reattaching streamline, we can write a momentum balance which will yield θ:

$$J\cos\theta = J_3 - J_2 \quad .$$

This equation assumes that the pressure forces and shear stress forces are small enough to be neglected. We shall check this assumption below.

The integrated momentum equation, as given in general, is

$$F_{BODY} = \iint_S (-P\vec{n} + \vec{\tau})\,dS - \iint_{S+\sigma'} \rho\vec{v}(\vec{v}\cdot\vec{n})\,dS - \iiint_V \frac{\partial}{\partial t}(\rho\vec{v})\,dV$$

where σ' is the surface area of the body contained within the control volume whose surface area is S and volume is V. For our case, we do not have a body in the control volume so the momentum equation becomes

$$\iint_S (-P\vec{n} + \vec{\tau} - \rho\vec{v}(\vec{v}\cdot\vec{n}))\,dS = 0 \quad .$$

We can now estimate the magnitudes of the three terms on each surface of the control volume and compare them.

Estimating the shear stress term, we note that

$$\vec{\tau} \sim \rho\varepsilon\frac{\partial u}{\partial y} \sim \rho\varepsilon\frac{U}{\delta} \quad .$$

But according to Schlichting,[4]

$$\varepsilon = 0.001372\,Ux$$

for turbulent shear layers and so $\vec{\tau} \sim 0.00516\rho U^2$ for $\sigma = 12$ and $\delta = \frac{3.19}{\sigma}x$. Thus on surfaces (1), (2), and (3) of the control volume, $\vec{\tau}$ should have a maximum value of $0.00516\rho U^2$. On surface (4), we can essentially assume that the integrated shear stress is less than $0.00516\rho U^2$ since the profile at the reattachment point should be a zero shear profile and the velocity profiles near this point should be low shear, low velocity forms.

To estimate the size of $P\vec{n}$, we should consider the maximum pressure difference that can occur on each surface. The greatest pressure difference should occur on (4) since this surface

extends from the separation cavity to a distance past the reattachment point. However, since we are interested in balancing forces in the x direction, the components of interest will be zero. On surfaces (2) and (1), the maximum pressure difference will be given by $P_\infty - P_c$ since these surfaces go from the cavity to a point outside of the jet. We have two ways to estimate this value. Using the data in Sawyer's paper, we see that $\frac{\Delta P}{J/h} = \bar{P} = 0.2$ for $h/t = 3$ gives the greatest value for $\Delta p = P_\infty - P_c$. This gives

$$\Delta p \sim \bar{p} \frac{\rho U^2 t}{h} \sim 0.067 \rho U^2 \quad .$$

For larger values of ΔP, we can extrapolate Sawyer's curve for $h/t \to 0$. Measuring the slope of the curve, we have $\Delta p \sim 0.08 \rho U^2$. Another way of estimating ΔP is to use data obtained in this present investigation. Extrapolating the curves of C_p vs. h/t, we see that $C_{p_{max}} = 0.2$ which leads to

$$\Delta p \sim 0.1 \rho U^2 \quad .$$

Since this is the largest value we have, we will say that $P\vec{n} \sim .1 \rho U^2$ on surfaces (1) and (2). Finally on surface (3), we will estimate the maximum pressure difference as $P_r - P_\infty$ where P_r is the peak recovery pressure on the ground plane. From Sawyer's data, $p_r - P_\infty \sim 0.145 \rho U^2$ and the present investigation gives $p_r - P_\infty \sim 0.13 \rho U^2$ so we have $P\vec{n} \sim 0.145 \rho U^2$ on surface (3).

Knowing the maximum values of $\vec{\tau}$ and $P\vec{n}$, we can now compare them with ρU^2 to determine the maximum error we should expect in our calculation of θ by using only the momentum balance. We find that the force balance uses 87% of the force components and

so has a maximum error of 13%. This error appears to be acceptable in view of the fact that the inclusion of the pressure forces in the computation adds a great deal of complication for only a slight correction. The pressure could have been estimated by

$$P_\infty - P = \frac{1}{R}\int_y^\infty \rho u^2 dy$$

and this expression could have been incorporated into the momentum balance equation. But R is a function of θ since $x_1 - x_o \cong R\theta$ and so the solution of θ would have involved an extra iteration.

Returning to the momentum balance equation, we can rewrite it as

$$\cos\theta = 1 - 2\frac{J_2}{J} \qquad \text{since} \quad J = J_3 + J_2 \quad .$$

Calculating the momentum below the reattaching streamline, we find

$$J_2 = \int_{-\infty}^{y_{R_1}} \rho u^2 dy = \rho U^2 \frac{x_1}{a\sigma}\left(T_1 - \frac{T_1^3}{3} + \frac{2}{3}\right)$$

where $T_1 = \text{TANH}(a\xi_{R_1} + b)$ and $\xi_{R_1} = \xi_R$ at $X = X_1$

and so $\text{Cos}\theta = 1 - \frac{1}{a\alpha(x_1)}\left(T_1 - \frac{T_1^3}{3} + \frac{2}{3}\right)$.

Since we previously had T as a function of $\alpha(x)$ and h/t, we need only find a relationship between h/t and $\alpha(x)$ to completely describe the global features of the flow field. We will now derive this relationship by considering the geometry of the flow.

4. Geometrical Relationships Involving Jet Thickness, Step Height, Bubble Length, and Cavity Pressure

Looking at figure 6, we can see that it should be possible to relate h, t, and ℓ to various other lengths such as R, y_R, and δ.

But since these latter parameters are known in terms of $\alpha(x)$ and h/t, we should be able to derive a set of equations which may be solved to give ℓ/h as a function of h/t.

From the figure, we can write

$$h+t = R - R\cos\theta + (t - \delta_{20} + \delta_{21})\cos\theta + \delta_{21} + y_{R_1}$$

where $\delta_{21} = \delta_2$ at $x = x_1$.

Notice that $\delta_{2_1} + y_{R_1}$ gives the difference between the two lengths since $\delta_{21} > 0$ and $y_{R_1} < 0$ because of the ways in which they have been defined. Since the radius of curvature of the shear layer centerline, R_o, equals $R-t + \delta_{20}$, we can write

$$h = R_o(1-\cos\theta) + \delta_{21}\left(\cos\theta + 1 + \frac{y_{R_1}}{\delta_{21}} - \frac{\delta_{20}}{\delta_{21}}\right) .$$

Using the momentum parameter, $\alpha(x_1)$, in the form

$$\frac{1}{t} = \frac{\sigma}{x_1(\alpha(x_1) - (0.053 - 1.09\frac{x_o}{x_1})\gamma)} \equiv \frac{\sigma}{x_1 J_*}$$

and $\frac{R_o}{x_1} = \frac{1 - \frac{x_o}{x_1}}{\theta}$, we can finally write

$$\frac{h}{t} = \frac{1}{J_*}\left(\frac{\sigma}{\theta}\left(1 - \frac{x_o}{x_1}\right)(1-\cos\theta) + 2.36\left(\cos\theta + 1 + \frac{\bar{y}'_{R_1}}{2.36} - 0.462\frac{x_o}{x_1}\right)\right).$$

This completes the set of equations which gives h/t as a function of $\alpha(x_1)$. If we can now write ℓ/h as a function of $\alpha(x_1)$, we will have completed the first half of the theoretical analysis.

However, before writing ℓ/h, we notice that a relationship giving ϕ as a function of known parameters will be needed, since it is obvious that ℓ depends upon ϕ. This relationship can be found by writing h/t in terms of ϕ and then equating this expression to the previous one we derived for h/t as a function of θ. From the

geometry, we can write

$$\frac{h}{t} = \frac{R_o}{t}(1-\cos\phi) + \frac{\delta_{22}}{t}\left(\cos\phi - \frac{\delta_{20}}{\delta_{22}}\right) \quad .$$

But $\frac{\delta_{20}}{\delta_{22}}$ contains $\frac{x_o}{x_2}$ which can be found by observing that $x_2 - x_1 = R_o(\phi-\theta)$. Thus

$$\frac{X_o}{X_2} = \frac{X_o/X_1}{1 + \frac{(1-\frac{X_o}{X_1})(\phi-\theta)}{\theta}} \quad .$$

Now we can equate the two expressions of h/t to give

$$\frac{\sigma}{\theta}\left(1-\frac{X_o}{X_1}\right)(\cos\phi-\cos\theta) + 2.36\left(\cos\theta + 1 + \frac{\zeta'_{R_1}}{2.36} - \left(1 + \frac{(1-\frac{X_o}{X_1})(\phi-\theta)}{\theta}\right)\cos\phi\right) = 0$$

and this gives us a way to calculate ϕ.

At this point we can write ℓ in terms of the known lengths in the problem:

$$\ell = (R - t + \delta_{20} - \delta_{22})\sin\phi + \frac{\delta_{22} + y_{R_2}}{\sin\phi} \quad .$$

This expression is only approximate since it assumes that the reattaching streamline is perpendicular to the radius R at $x = x_2$ and that the streamline is very nearly straight from x_2 until it impinges upon the ground plane.

The expression for ℓ requires $\alpha(x_2)$ since

$$\zeta'_{R_2} = \frac{\sigma y_{R_2}}{X_2} = \sqrt{1.266 - 1.22\sqrt{\frac{\alpha(x_2)\,X_o}{\alpha(x_o)\,X_2}}} - 1.36 \quad .$$

However, by manipulating $\alpha(x_2) = \frac{\sigma t}{x_2} + (0.053 - 1.09\frac{x_o}{x_2})\gamma$ and $x_2 = x_1 + R_o(\phi-\theta)$, we find

$$\alpha(x_2) = \alpha(x_1) - \frac{(\alpha(x_1) - 0.053\gamma)}{1 + \frac{\theta}{(1-\frac{x_o}{x_1})(\phi-\theta)}} \quad .$$

By writing $\frac{\ell}{h} = \frac{\ell}{t}\frac{t}{h}$ and finding $\frac{\ell}{t}$, we will be able to calculate $\frac{\ell}{h}$. The expression for $\frac{\ell}{t}$ is

$$\frac{\ell}{t} = \frac{1}{J_*}\left(\frac{\sigma}{\theta}\left(1-\frac{x_0}{x_1}\right)\sin\phi + \left(1+\frac{\left(1-\frac{x_0}{x_1}\right)(\phi-\theta)}{\theta}\right)\left(\frac{2.36+\bar{\xi}'_{R2}}{\sin\phi} - 2.36\sin\phi\right)\right)$$

and this completes the first half of the theoretical analysis for calculating the bubble length as a function of jet thickness.

However, for completeness, we should try to estimate the behavior of the cavity pressure as a function of the jet thickness. We would expect that the pressure estimation should not be as accurate as the bubble length calculation. This is due to the fact that the pressure difference equation,

$$\Delta P = \frac{J}{R} = \frac{1}{R}\int_{-\infty}^{\infty} \rho u^2\, dy \quad ,$$

is really only approximately true and, while it is used only indirectly in the bubble length calculation, it is fundamental in predicting the cavity pressure. It is more accurate to write the pressure difference equation as

$$\Delta P = \int_{\delta_2}^{\delta_{2u}} \frac{\rho u^2}{R+y}\, dy = \frac{1}{R}\int_{\delta_2}^{\delta_{2u}} \frac{\rho u^2}{1+\frac{y}{R}}\, dy \quad ,$$

and for very thin jets, this expression approaches the previous one. However for large jet thicknesses, this equation gives a smaller value of ΔP owing to the fact that the integrand is reduced by the denominator over the range of integration. Thus we would expect to find that the calculated cavity pressures will be larger than the experimental values especially for large jet thicknesses.

In Sawyer's papers,[2, 3] he presented the cavity pressure, P_c, in the form of a pressure coefficient based upon the jet momentum: $\frac{\Delta P}{J/h}$. This value can easily be calculated since

$$\frac{\Delta P}{J/h} \equiv \overline{P} = \frac{h}{R} = \frac{R_o}{R}(1-\cos\theta) + \frac{\delta_{21}}{R}\left(\cos\theta + 1 + \frac{\xi'_{R_1}}{2.36} - 0.462\frac{x_o}{x_1}\right).$$

But $$\frac{R_o}{R} = \frac{1}{1+\frac{\theta}{\sigma}\left(\frac{J_* - 1.09\frac{x_o}{x_1}}{1-\frac{x_o}{x_1}}\right)},$$

So $$\frac{\Delta P}{J/h} \equiv \overline{P} = \frac{\sigma(1-\frac{x_o}{x_1})(1-\cos\theta) + 2.36\theta\left(\cos\theta + 1 + \frac{\xi'_{R_1}}{2.36} - 0.462\frac{x_o}{x_1}\right)}{\sigma(1-\frac{x_o}{x_1}) + \theta\left(J_* - 1.09\frac{x_o}{x_1}\right)}.$$

However, $\overline{P}$ goes to zero as h/t goes to zero since the jet momentum becomes infinite. Therefore, since we are interested in jet thicknesses several times the step height, it is better to present the cavity pressure as

$$C_p = \frac{\Delta P}{\frac{1}{2}\rho U_o^2}.$$

Combining this equation with the previous one, we obtain

$$C_p = 2.08\,\alpha(x_o)\frac{\delta_o}{h}\overline{P} \qquad \text{for} \quad \frac{\delta_o}{h} \text{ constant}$$

or $$C_p = 2.08\,\alpha(x_o)\frac{\delta_o}{t}\frac{t}{h}\overline{P} \qquad \text{for} \quad \frac{\delta_o}{t} \text{ constant}.$$

This completes the analysis of the problem of calculating the bubble length and cavity pressure as a function of the jet thickness without the effect of the spanwise blowing jet.

B. Effect of Spanwise Blowing on Separation Bubble

In order to account for the effect of the spanwise blowing jet, we shall approximate its influence by a two-dimensional sink with sink strength given by $d\dot{q}_j/dz$ where $\dot{q}_j$ is the volume flow per unit length of the spanwise blowing jet. Since $\dot{q}_j$ is linear in z where z is the distance along the jet axis from the jet nozzle, $d\dot{q}_j/dz$ is a con-

stant. Let us call $d\dot{q}_j/dz = \dot{q}_s$. This is the volume flow per unit time that the jet entrains.

The preceding analysis should remain intact except that the mass balance relationship which gave the reattaching streamline will now change. The new reattaching streamline will be defined as that streamline, coming from upstream, under which all the fluid is fed into the separation bubble and the sink, and above which all the fluid continues downstream. Looking at figure 7, we can see that $\dot{q}_{1b} = \dot{q}_s$ will define the height of the reattaching streamline at $x = x_o$. Then by doing a mass balance between the streamline, $\xi = 0.125$, in the upper shear flow and the reattaching streamline at $x = x_o$, the reattaching streamline can be defined for all x.

Let us define $\dot{q}_s = \mu \dot{q}_1$. Then since $\dot{q}_{1a} + \dot{q}_{1b} = \dot{q}_1$, we have

$$\dot{q}_{1a} = \dot{q}_1 (1 - \mu) \quad .$$

Using this equation, we can put in $\dot{q}_{1a}$ for an arbitrary x and write $\dot{q}_1$ for $x = x_o$, and this will define ξ_R.

Now $\dot{q}_1$ is the volume flow between $\xi = -0.73$ of the lower shear layer and $\xi = 0.125$ of the upper shear layer, so

$$\dot{q}_1 = \frac{U_o x_o}{\sigma} \left[\frac{0.896}{a} + \frac{0.666}{a v} + 2 \left(\frac{\sigma t}{x_o} - 1.92 \gamma \right) \right] .$$

Before calculating $\dot{q}_{1a}$, we observe that this quantity must be calculated in two different ways depending upon whether the reattaching streamline lies above or below the upper boundary of the lower shear layer. Defining $\dot{q}_*$ as the volume flow between the streamline of the upper shear layer ($\xi = 0.125$) and the upper boundary of the lower shear layer, we find

$$\dot{q}_* = \frac{Ux}{\sigma}\left(\frac{0.666}{a\nu} + 2\left(\frac{\sigma t}{x} - 1.09\gamma\frac{x_o}{x} - 0.83\gamma\right)\right) .$$

This volume flow will vary as a function of x since it is not bounded by two streamlines. If $\dot{q}_{1a} > \dot{q}_*$, we have to integrate into the lower shear layer and if $\dot{q}_{1a} < \dot{q}_*$, we do not have to integrate into the shear layer. By defining the quantity $\mu^* = 1 - \frac{\dot{q}_*}{\dot{q}_1}$, we can specify the two forms of $\dot{q}_{1a}$ by $\mu < \mu^*$ or $\mu > \mu^*$.

It is apparent that $\mu < \mu^*$ marks the condition for which $\dot{q}_{1a}$ is integrated into the shear layer and this condition is of greater interest to us since this will include $\mu = 0$. The quantity μ^* will first be calculated since both $\dot{q}_1$ and $\dot{q}_*$ are already known:

$$\mu^* = \frac{0.23\left(\frac{U_o x_o}{Ux}\right) + 0.666}{\frac{U_o x_o}{Ux}\left(0.896 + \frac{0.666}{\nu} + 2a\left(\frac{\sigma t}{x_o} - 1.92\gamma\right)\right)} .$$

So for $\mu < \mu^*$, we have

$$\dot{q}_{1a} = \frac{Ux}{\sigma}\left[\frac{0.666}{a\nu} - \frac{T}{a} + 2\left(\frac{\sigma t}{x} - \gamma\left(1.09\frac{x_o}{x} + 0.83\right)\right)\right] .$$

Equating this with $\dot{q}_1(1-\mu)$, we obtain the expression for ξ_R:

$$T = \frac{U_o x_o}{Ux}\left(\mu\left(2a\left(\frac{\sigma t}{x_o} - 1.92\gamma\right) + \frac{0.666}{\nu} + 0.896\right) - 0.23\right) - 0.666$$

where $T = \tanh(a\xi_R + b)$. Notice that the expression reduces to the one found previously without the spanwise blowing jet when $\mu = 0$. Rewriting T in a slightly more usable form, we have

$$T = \sqrt{\frac{\alpha(x)x_o}{\alpha(x_o)x}}\left(\mu\left(2.9\left(\frac{h}{\delta_o}\frac{t}{h} - \gamma\right) + \frac{0.666}{\nu} + 0.896\right) - 0.23\right) - 0.666 \qquad (\mu < \mu^*)$$

for $\frac{\delta_o}{h}$ = constant

or $$T = \sqrt{\frac{\alpha(x)x_o}{\alpha(x_o)x}}\left(\mu\left(2.9\left(\frac{t}{\delta_o} - \gamma\right) + \frac{0.666}{\nu} + 0.896\right) - 0.23\right) - 0.666 \qquad (\mu < \mu^*)$$

for $\frac{\delta_o}{t}$ = constant.

As before, we see that it is difficult to use the form of the inverse hyperbolic tangent when solving for ξ'_R so we will again approximate u/U by $1/2(1+\xi)$. The use of this expression here is not as accurate as its use in the previous section; however the inaccuracy may be minimized by avoiding large values of μ near μ^*. Using this approximation, we find that ξ'_R is given by

$$\xi'_R = \sqrt{5.3T + 4.8} - 1.36 \qquad \text{for } \mu < \mu^*.$$

For large amounts of mass entrainment, we have to consider $\dot{q}_{1a}$ for $\mu > \mu^*$:

$$\dot{q}_{1a} = \frac{Ux}{\sigma}\left(\frac{0.666}{a\nu} + 2\left(\frac{\sigma t}{x} - 1.09\gamma\frac{x_o}{x}\right) - \frac{0.83}{\nu} - \xi'_R\right) .$$

Again, we equate this to $\dot{q}_1(1-\mu)$ and find

$$\xi'_R = \frac{U_o x_o}{Ux}\left(\mu\left(\frac{0.896}{a} + \frac{0.666}{a\nu} + 2\left(\frac{\sigma t}{x_o} - 1.92\gamma\right)\right) - \frac{0.23}{a}\right) - \frac{0.666}{a} + 0.83 \qquad \text{for } \mu > \mu^*.$$

Since ξ'_R has been found directly, it is an easy matter to determine T since $T = \tanh(a\xi_R + b)$:

$$T = \text{TANH}\left(a\left(\xi'_R + 0.36\right) + b\right) \qquad \text{for } \mu > \mu^*.$$

Both ξ'_R and T should approach the same values for the cases of $\mu > \mu^*$ and $\mu < \mu^*$ when $\mu = \mu^*$. At $\mu = \mu^*$, $\xi'_R = 0.83$ and $T = 0$ so both expressions become

$$0 = \frac{U_o x_o}{Ux}\left(\mu\left(0.896 + \frac{0.666}{\nu} + 2a\left(\frac{\sigma t}{x_o} - 1.92\gamma\right)\right) - 0.23\right) - 0.666 .$$

It is interesting to note that even the approximate ξ'_R derived for $\mu < \mu^*$ becomes 0.83 when $\mu = \mu^*$. So this approximation appears to be not as bad as previously thought.

This completes the analysis since this gives the reattaching

streamline as a function of the mass entrainment. However, for convenience, we would like to be able to specify $\dot{q}_s$ and have this define μ so we shall solve for μ as a function of $\dot{q}_s$. This is a relatively simple task since it merely involves expanding $\mu = \dot{q}_s/\dot{q}$, into more usable forms:

$$\mu = \frac{1.45\ \overline{K}}{0.896 + \frac{0.666}{\nu} + 2.9\left(\frac{h}{\delta_o}\frac{t}{h} - \gamma\right)} \qquad \text{where } \overline{K} = \frac{\dot{q}_s}{U_o \delta_o}$$

$$\text{for } \frac{\delta_o}{h} = \text{constant}$$

or

$$\mu = \frac{1.45\ \overline{K}}{0.896 + \frac{0.666}{\nu} + 2.9\left(\frac{t}{\delta_o} - \gamma\right)}$$

$$\text{for } \frac{\delta_o}{t} = \text{constant}.$$

However, it would be even better to normalize $\dot{q}_s$ with Q_o, the total volume flow coming from the two-dimensional jet. We know that

$$Q_o = \dot{q}_1 + \int_{\xi=-0.73}^{\xi=0.125} u\,dy$$

where the integral is taken over the upper shear layer. Thus we have

$$Q_o = \dot{q}_1 + 0.23\,\frac{U_o x_o}{a\sigma_1}$$

Taking $\frac{\dot{q}_s}{Q_o} = \frac{\dot{q}_s/\dot{q}_1}{1 + 0.23\,\frac{U_o x_o}{a\sigma_1 \dot{q}_1}}$, we have μ as a function of $\dot{q}_s/Q_o$:

$$\mu = \frac{\dot{q}_s}{Q_o}\left(1 + \frac{0.23/\nu}{0.896 + \frac{0.666}{\nu} + 2.9\left(\frac{h}{\delta_o}\frac{t}{h} - \gamma\right)}\right)$$

$$\text{for } \frac{\delta_o}{h} = \text{constant}$$

or

$$\mu = \frac{\dot{q}_s}{Q_o}\left(1 + \frac{0.23/\nu}{0.896 + \frac{0.666}{\nu} + 2.9\left(\frac{t}{\delta_o} - \gamma\right)}\right)$$

$$\text{for } \frac{\delta_o}{t} = \text{constant}.$$

This ends the theoretical analysis. Presumably, it should now be possible to predict the length of the separation bubble as a function of the two-dimensional jet thickness with and without the spanwise blowing jet.

III. Experimental Investigation

An experiment was conducted to test the validity of several of the assumptions used in the analysis, and also to verify the behavior of the bubble length as a function of the spanwise jet blowing and the two-dimensional jet thickness as predicted by the theory. Moreover, since the theory is based upon the spreading of a turbulent jet, the spreading parameter, σ, is left undetermined and so it is necessary to conduct an experiment to determine its magnitude.

A. Experimental Setup

In order to create the effect of a two-dimensional jet blowing past a rearward facing step, a plenum chamber with a jet slot and a ground plane were built to the specifications shown schematically in figure 8. The air flow was provided by two five horsepower blowers which were connected to the bottom of the plenum chamber. The jet slot had a width of 30 inches and a variable thickness which ranged from zero to 5.70 inches. Pressure taps, connected to a butyl alcohol multimanometer, were located at various positions in the ground plane which could also be varied to give different step heights. Side plates were provided to help contain the flow and to approximate two-dimensional conditions.

The spanwise jet was created by taking air from the compressed air line and running it through a 0.14 inch inner diameter tube mounted flush against the corner formed by the step and the ground plane. Splitter plates were used to minimize the three-dimensional cross flow effects induced by the spanwise blowing jet.

The jet was introduced through a hole in one of the plates and allowed to exit through a larger hole in the other plate with care taken to insure that the larger hole in the splitter plate was always below the reattaching streamline surface.

Prior to starting the experiment, vertical velocity profiles were taken at the edge of the jet slot at various stations along the width of the jet to check for the two dimensionality of the flow. Figure 9 shows a typical plot and it can be seen that the velocity variations are greatest in the boundary layer and vary less than one percent in the core flow.

As a final check on the flow conditions, tufts were used to determine the flow direction and to insure that there were no unexpected separation regions or areas of secondary flow to distort the experimental results.

B. Experimental Measurements

The measurement of primary importance was the separation bubble length and it was determined in two different ways. The first method employed was pitot measurements at the ground plane surface. An upstream facing pitot tube was moved parallel to the flow direction and pressure measurements were recorded. The pitot was then turned to face the downstream direction and similar measurements were taken. When the data were plotted as pressure versus the distance from the step base, the lines crossed at the location of the reattachment point. The second method employed to determine the reattaching distance was the use of tufts on the ground plane. By observing the flow direction, it was a relatively

simple matter to determine the reattachment line. The maximum disagreement between the two methods was about three percent and so it was decided that all subsequent measurements would be taken by using the tufts on the ground plane. It was also observed that the reattachment distance seemed to remain constant within two percent for measurements taken within the two-dimensional flow region.

In addition to measuring the separation bubble length, the pressure distribution on the ground plane and the boundary layer profiles were taken with each run. Figure 10 shows the boundary layer profile measurements suitably normalized. The velocities measured throughout the experiment were taken with a total head tube connected to a butyl alcohol manometer. All of the experiments were run with a Reynolds number, Re_{δ_*}, between 2200 and 6330 where Re_{δ_*} is the Reynolds number based on the displacement thickness. This is comparable to Sawyer's experiments which were conducted with $Re_{\delta_*} \approx 2400$.

Whenever the spanwise jet was used, a Brooks Rotameter flowmeter was employed to measure the volume flow of air being fed to the 0.14 inch tube.

C. Comparison of the Theoretical with the Experimental Results

Using the data obtained from the experiment, various curves were plotted to compare these results with the theory. A listing of the experimental results is shown in Table I.

A plot of C_p versus $h/2t$, shown in figure 11, reveals that the theory matches the experiment only for small jet thicknesses

and it begins to deviate quite a bit for h/2t less than 4. This type of behavior was expected because of the approximation made that $\Delta p = \frac{J}{R}$ instead of using

$$\Delta p = \frac{1}{R} \int_{\delta_2}^{\delta_{2u}} \frac{\rho u^2}{1 + \frac{y}{R}} \, dy \quad .$$

Therefore since we are primarily interested in larger jet thicknesses, we will no longer consider the pressure in the cavity as a function of jet thickness for the experiments run with the spanwise blowing jet.

Looking at figure 12, we have ℓ/h versus h/2t without the spanwise blowing jet. The trend of the data matches that of Sawyer for large h/2t and seems to approach the limit of infinite jet thicknesses, i.e., the flow past a rearward facing step in an infinite flow, as given by Tani.[6] The theoretical curves appear to match the data quite well for $\sigma = 15$, $\nu = 2/3$, and δ_o/t ranging from 0.2 to 0.4. Throughout the experiment, it was noted that δ_o/t tended to be about 0.4 for larger values of h/2t and that it approached 0.2 for the smaller values of h/2t. Thus, as expected, the curve for $\delta_o/t = 0.4$ matches the data better for large h/2t and the smaller values of δ_o/t are required to match the data for $h/2t \to 0$.

Finally, in dealing with the effect of the spanwise blowing jet on the separation bubble length, it was found that it was easier to use $\overline{K} = \frac{\dot{q}_s}{U_o \delta_o}$ as indicative of the mass entrainment of the jet instead of $\dot{q}_s/Q_o$. The latter parameter required complete velocity profiles across the two-dimensional jet slot and a graphical integration of these profiles while the use of $\overline{K}$ only required the boundary

layer thickness at the jet slot edge. However in both cases, it was necessary to make some statement about the volume flow entrained by the spanwise blowing jet. Since the jet was mounted flush against the corner, the volume flow entrainment should be greatly reduced as indicated by Abramovich[7] in his work with two-dimensional wall jets. As a test of this statement, an experiment was run for $h/2t = 4.3$ with the jet in the corner and with the jet removed approximately 1.95 inches from the nearest surface. In the first case, ℓ/h was found to be 1.68 and the second case gave $\ell/h = 1.41$. Although it is difficult to make a quantitative statement about this test, it is obvious that the entrainment was increased when the wall effects were lessened. However it was impossible to remove the jet sufficiently from the walls in order to attain the entrainment of a free jet and still be within the separation bubble and therefore it was decided to conduct all the experiments with the jet mounted flush against the corner.

During the actual experiments, the parameter

$$\mathcal{K} = \frac{q_{oj}}{r_j} \frac{1}{U_o \delta_o}$$

with $r_j = 0.14/2$ inches and

q_{oj} = volume flow issuing from jet nozzle

was kept constant and was used to indicate the entrainment of the jet. This was done because this parameter is directly proportional to the entrainment and it was difficult to determine exactly what the proportionality constant was experimentally. Two sets of data were obtained for

$$\frac{q_{oj}}{r_j} \frac{1}{U_o \delta_o} = 21.5 \text{ and } 10.75.$$

Looking at the experimental points in figures 13 and 14, we can see the effect of this mass entrainment.

Using the theoretical curves for $\sigma = 15$, $\nu = 2/3$, and $\frac{\delta_o}{t}$ ranging from 0.3 to 0.4, it was found that a value of $\overline{K} = 0.1$ was needed to match the data for $\mathcal{K} = 10.75$ and $\overline{K} = 0.2$ was required for $\mathcal{K} = 21.5$. But since $\overline{K} = C\mathcal{K}$ where C is the proportionality constant of the entrainment, we find that $C = 0.0093$ for both cases. However, according to Schlichting,[4] the constant for the entrainment due to a free jet is 0.228 if one assumes a top hat profile at the nozzle exit and thus we see that the entrainment of the semi-confined jet is reduced by a factor of 0.0408. An attempt was made to measure or at least estimate the volume flow entrained by the jet in the corner by taking velocity measurements at different stations downstream of the jet. These velocity fields were then integrated graphically to give the volume flow at various stations and thus the entrainment could be estimated. However, owing to the inaccuracy of the measurements and the graphical integration and also to the fact that the entrained flow was so small, it was impossible to make more than a qualitative statement about the entrainment. From these measurements, one can only say that it is possible that the flow entrainment constant is approximately 0.0093; however one cannot be sure about the actual magnitude.

REFERENCES

1. Dixon, C. J., "Lift Augmentation by Lateral Blowing over a Lifting Surface," AIAA Paper #69-193, February 1969.

2. Sawyer, R. A., "The Flow due to a Two-Dimensional Jet Issuing Parallel to a Flat Plate," Journal of Fluid Mechanics, Vol. 9, 1960, pp. 543-561.

3. Sawyer, R. A., "Two-Dimensional Reattaching Jet Flows Including the Effects of Curvature on Entrainment," Journal of Fluid Mechanics, Vol. 17, 1963, pp. 481-498.

4. Schlichting, Hermann, Boundary-Layer Theory, McGraw-Hill, Inc., New York, 1968, Chapter 24.

5. Liepmann, Hans and Laufer, John, "Investigations of Free Turbulent Mixing," NACA TN #1257, 1947.

6. Tani, Itiro; Iuchi, Matsusaburo; and Komoda, Hiroyuki, "Experimental Investigation of Flow Separation Associated with a Step or a Groove," Report of the Aeronautical Research Institute, University of Tokyo, Report #364, April 1961, pp. 119-136.

7. Abramovich, G. N., The Theory of Turbulent Jets, The Massachusetts Institute of Technology Press, Cambridge, 1963, Chapter 11.

LIST OF FIGURES

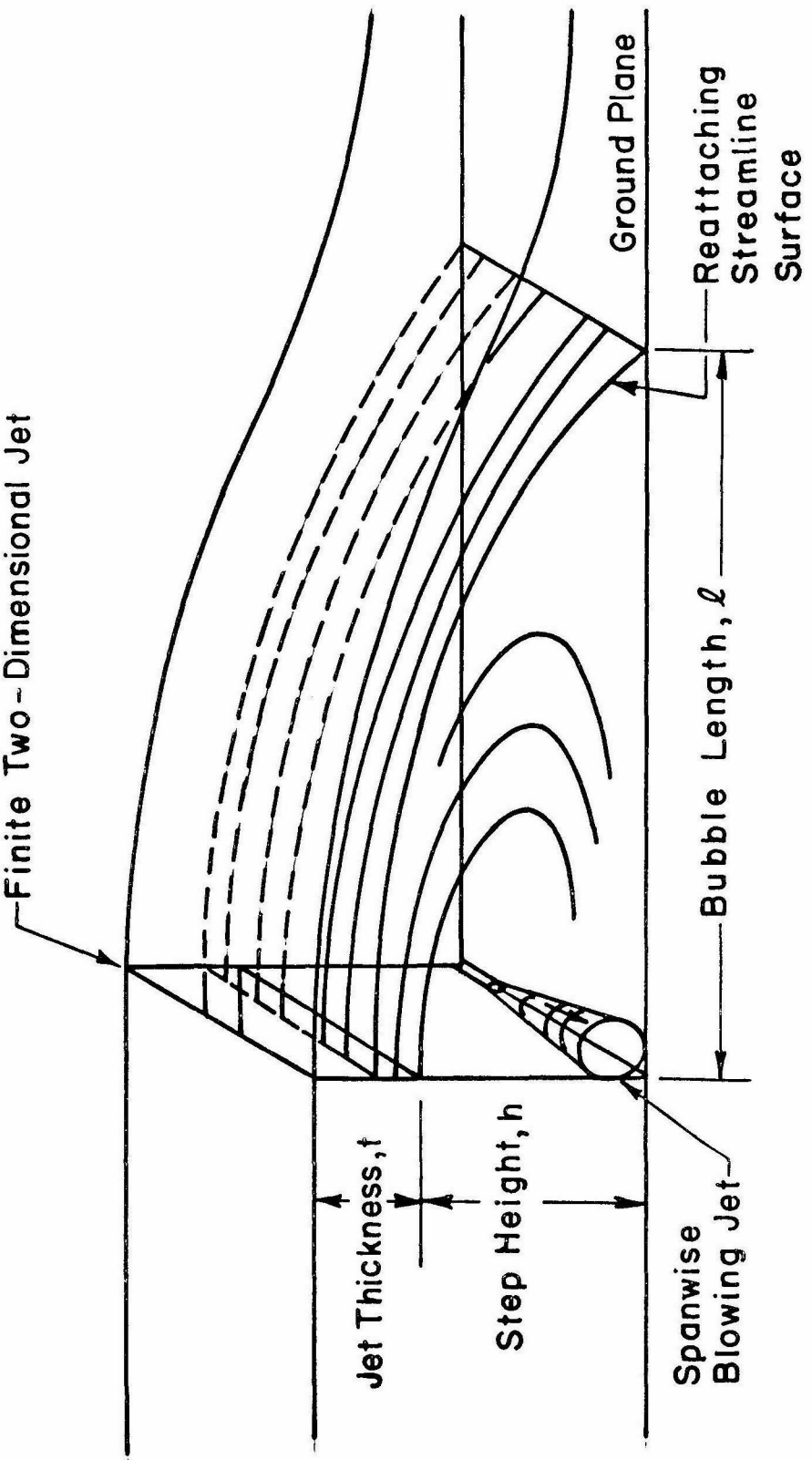

FIG. 1 SCHEMATIC OF FLOW CONFIGURATION

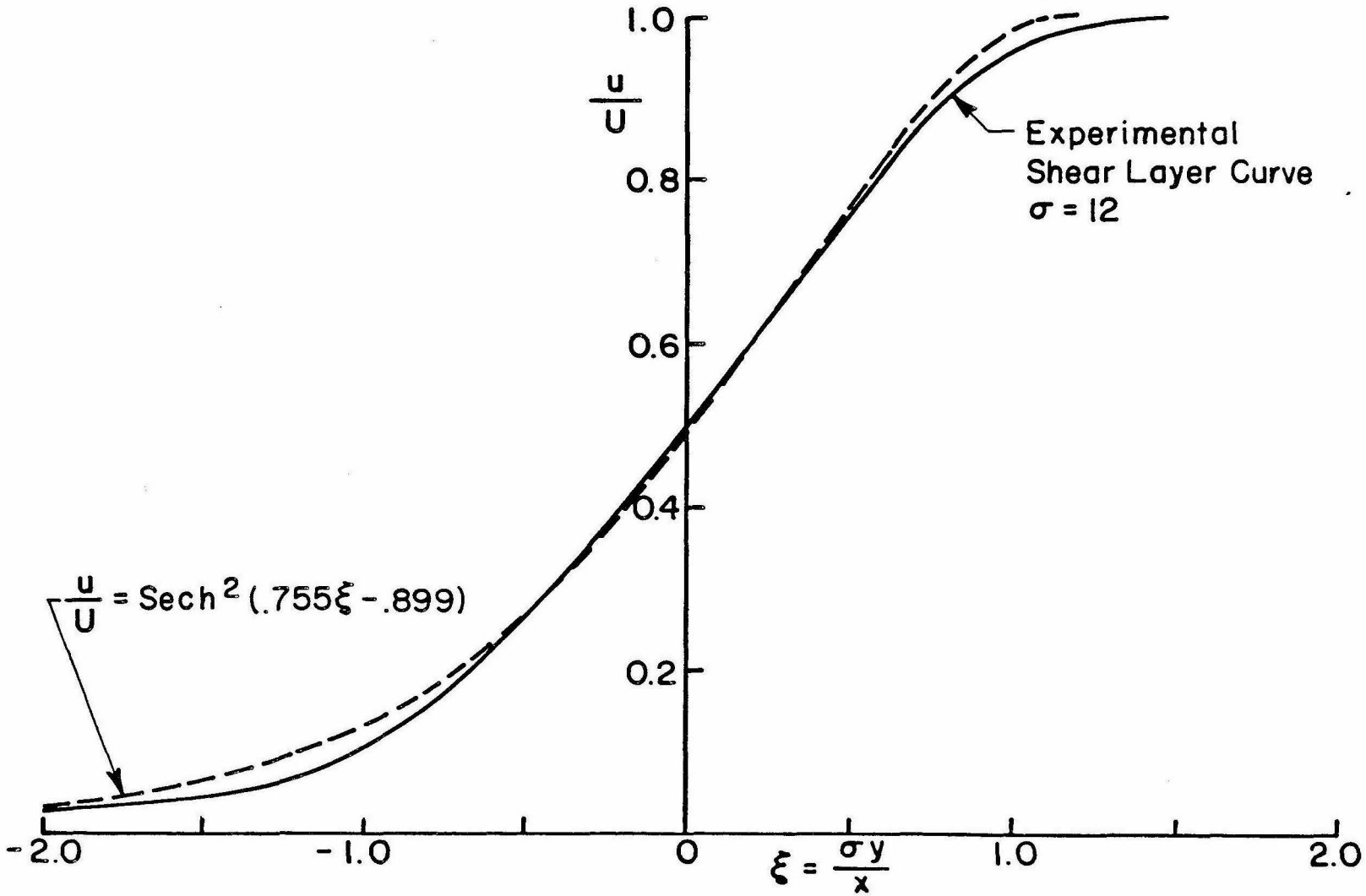

FIG. 2 SHEAR LAYER APPROXIMATION

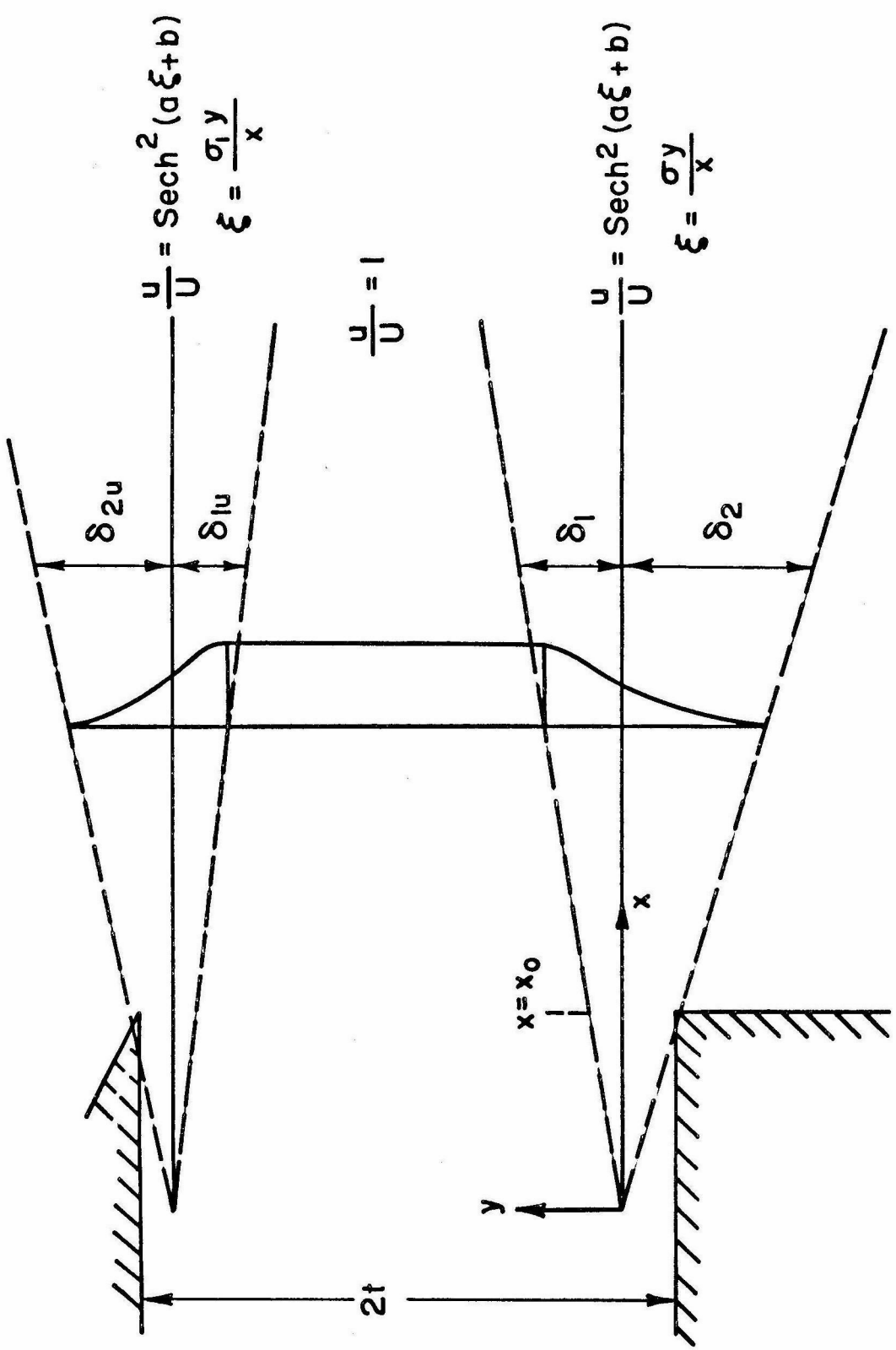

FIG. 3 TWO-DIMENSIONAL JET PROFILE

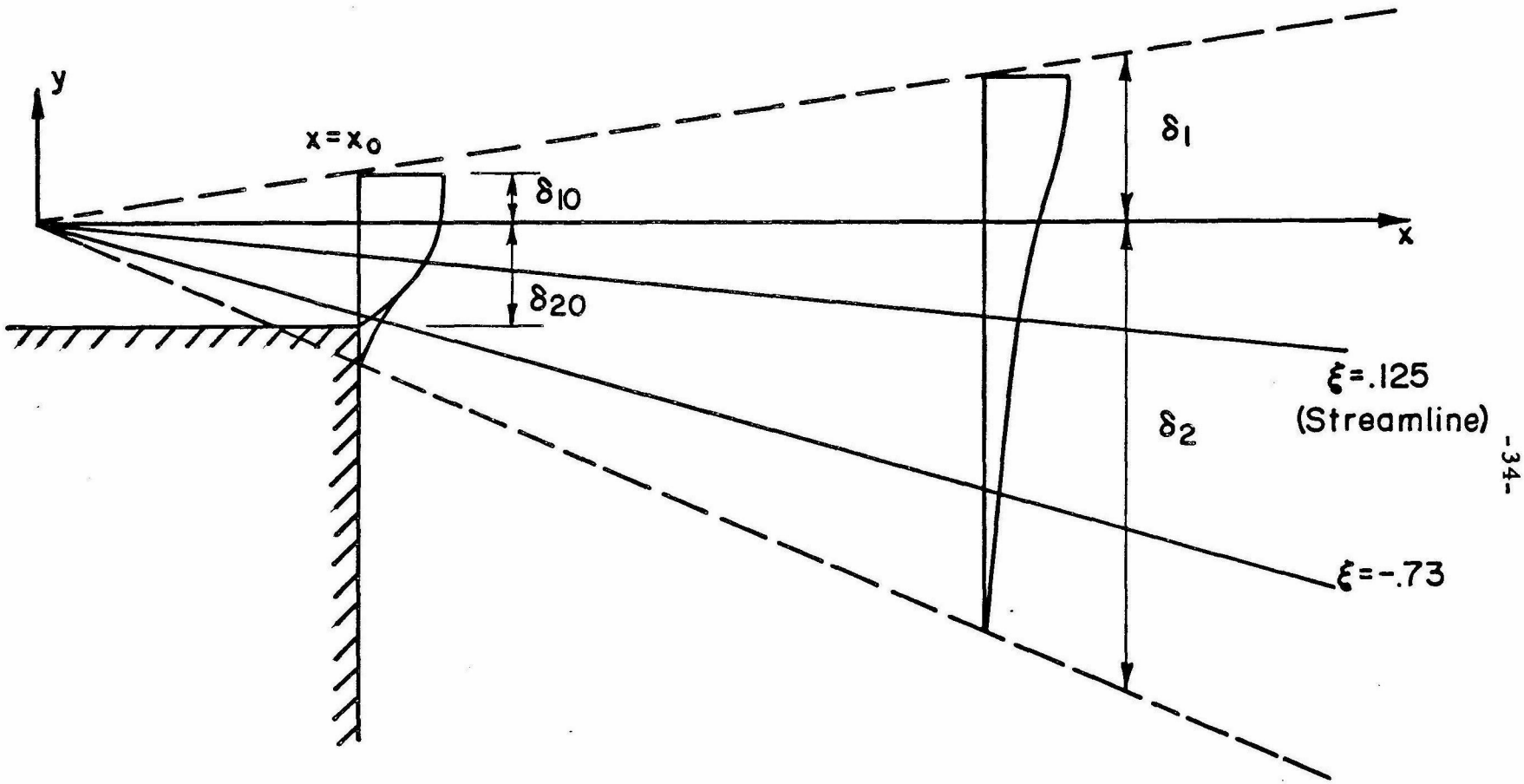

FIG. 4 SHEAR LAYER NEAR TWO-DIMENSIONAL JET SLOT EDGE

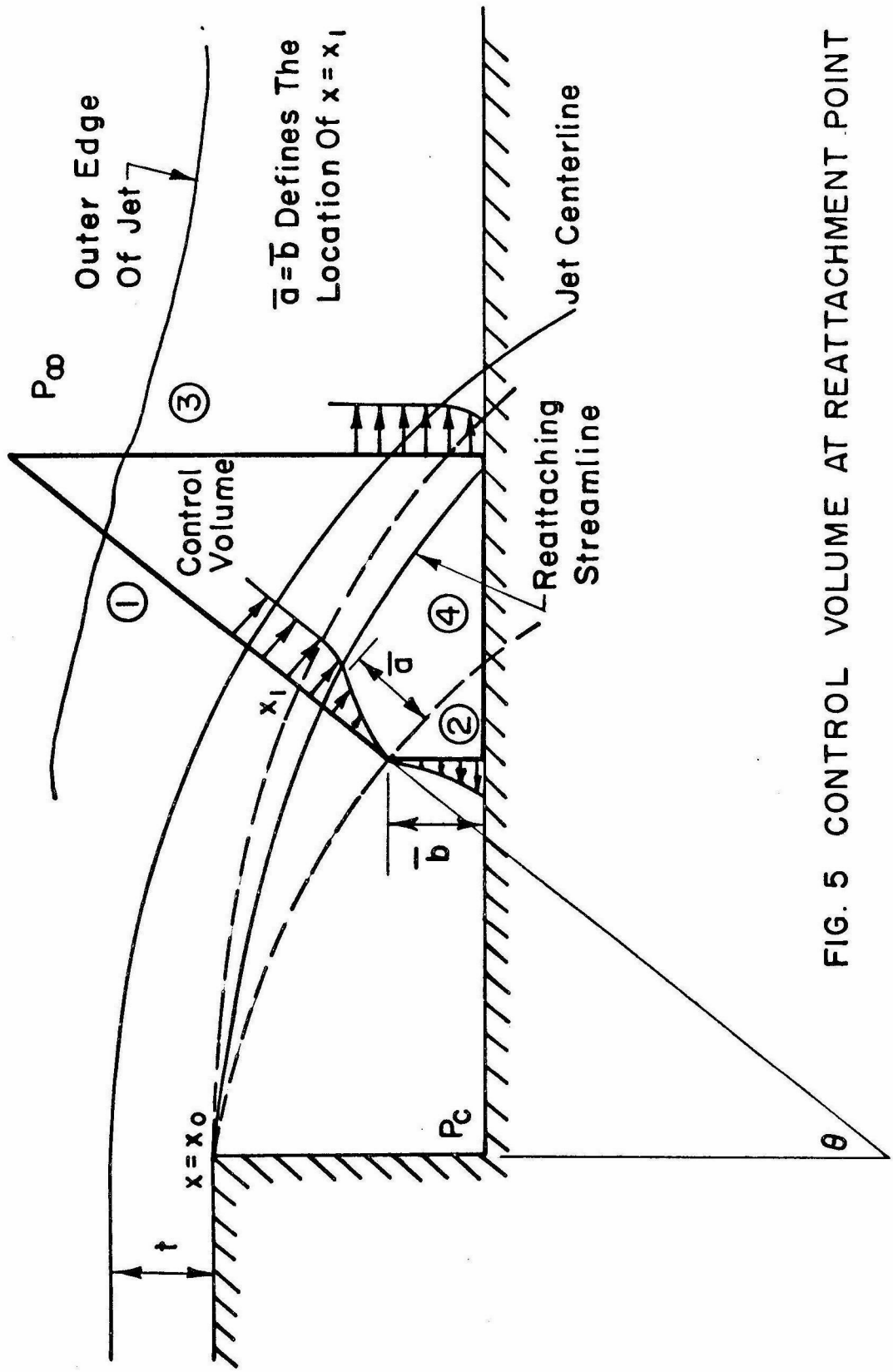

FIG. 5 CONTROL VOLUME AT REATTACHMENT POINT

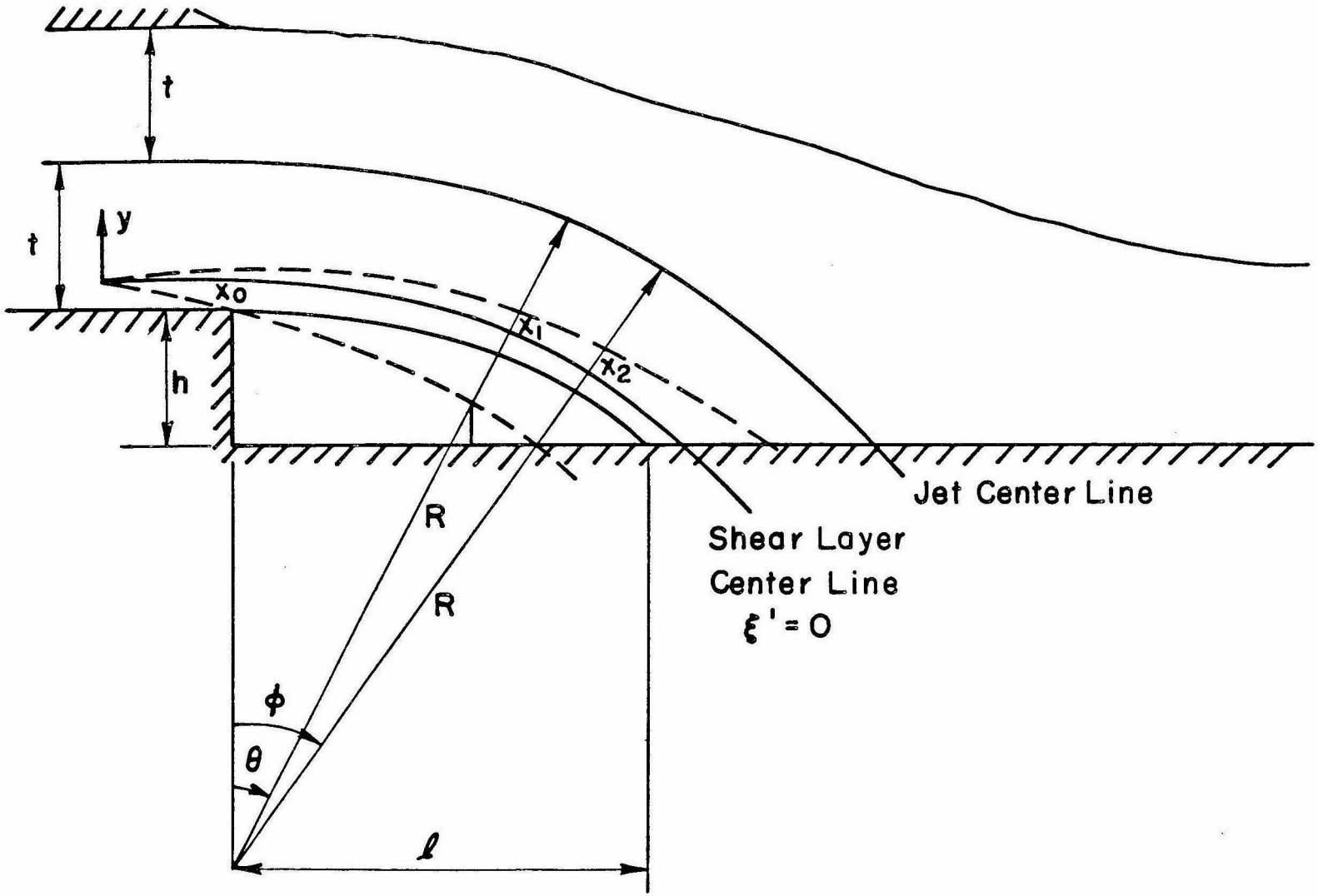

FIG. 6 SEPARATION BUBBLE GEOMETRY

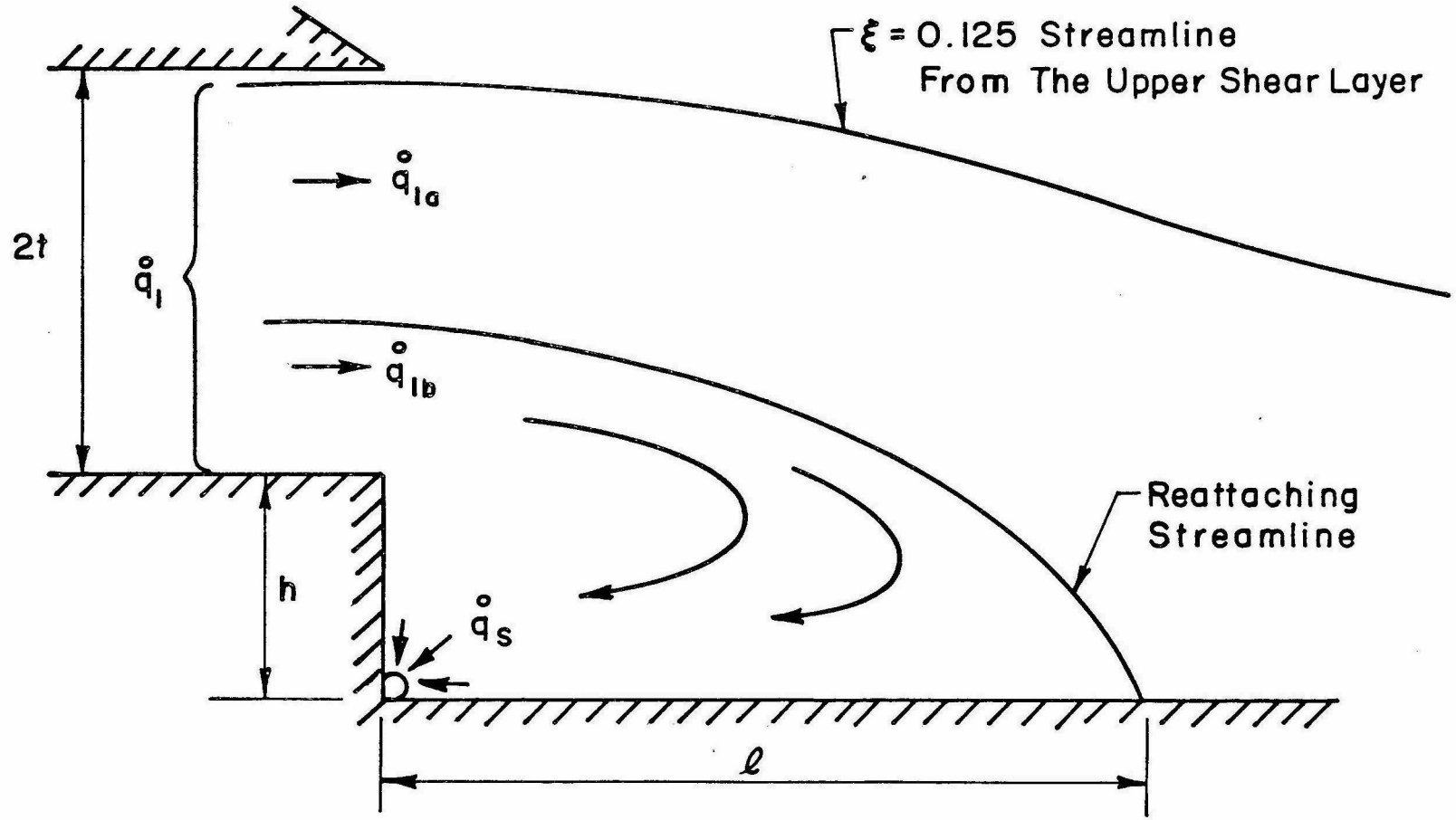

FIG. 7 REATTACHING STREAMLINE WITH SPANWISE BLOWING JET

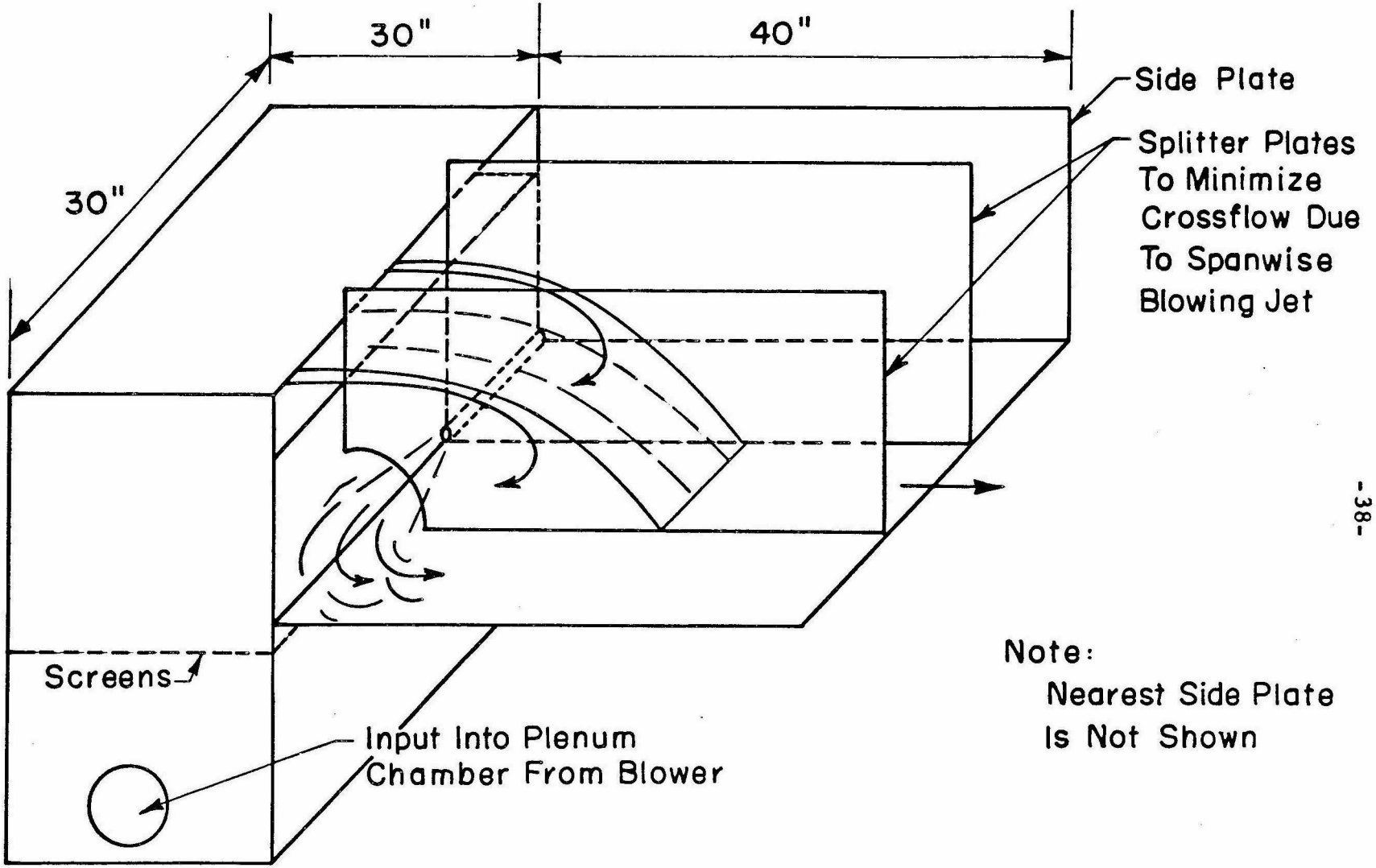

FIG. 8 SCHEMATIC OF EXPERIMENTAL SET-UP

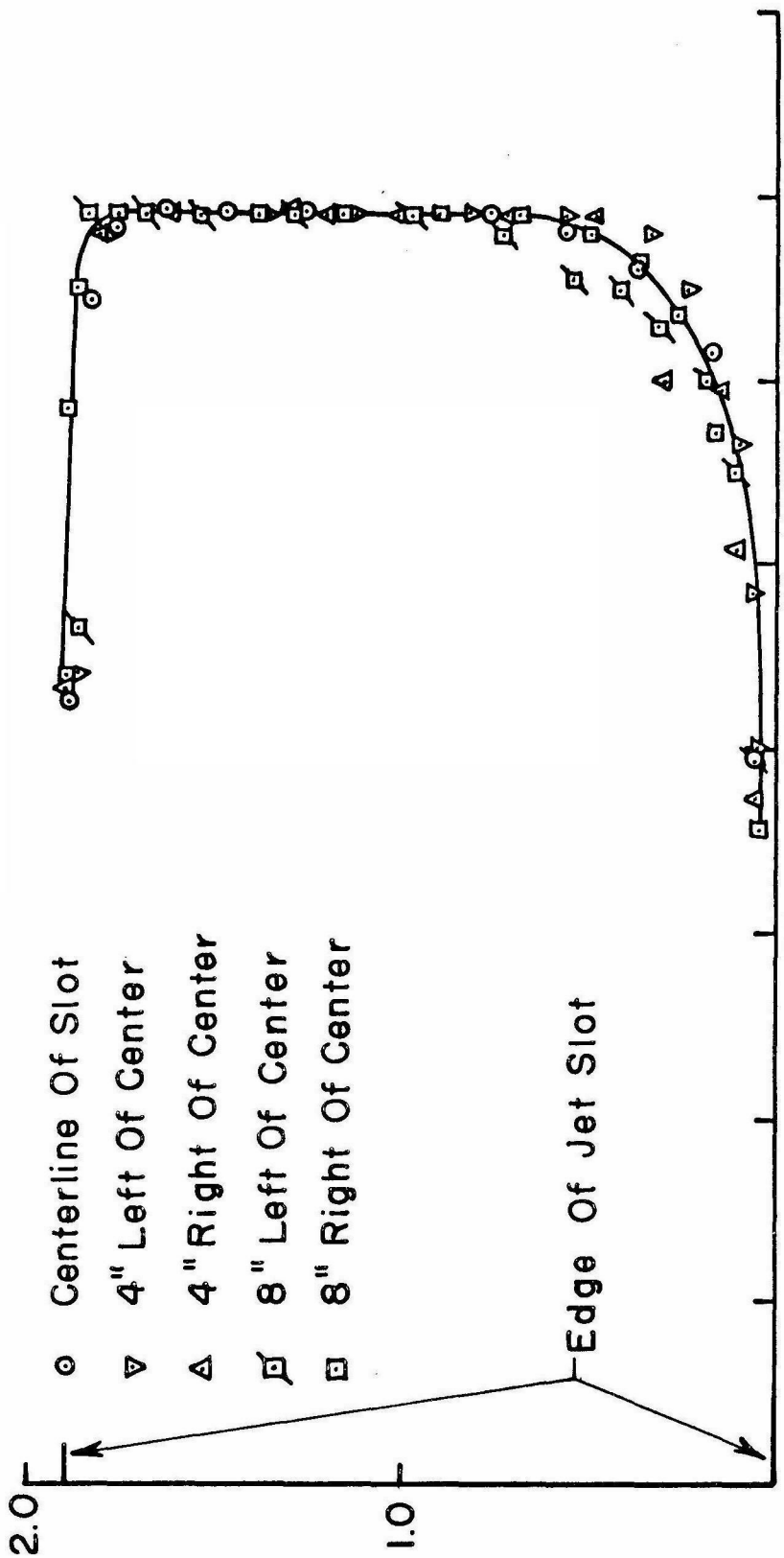

FIG. 9 VERTICAL VELOCITY PROFILES AT EDGE OF TWO-DIMENSIONAL JET SLOT

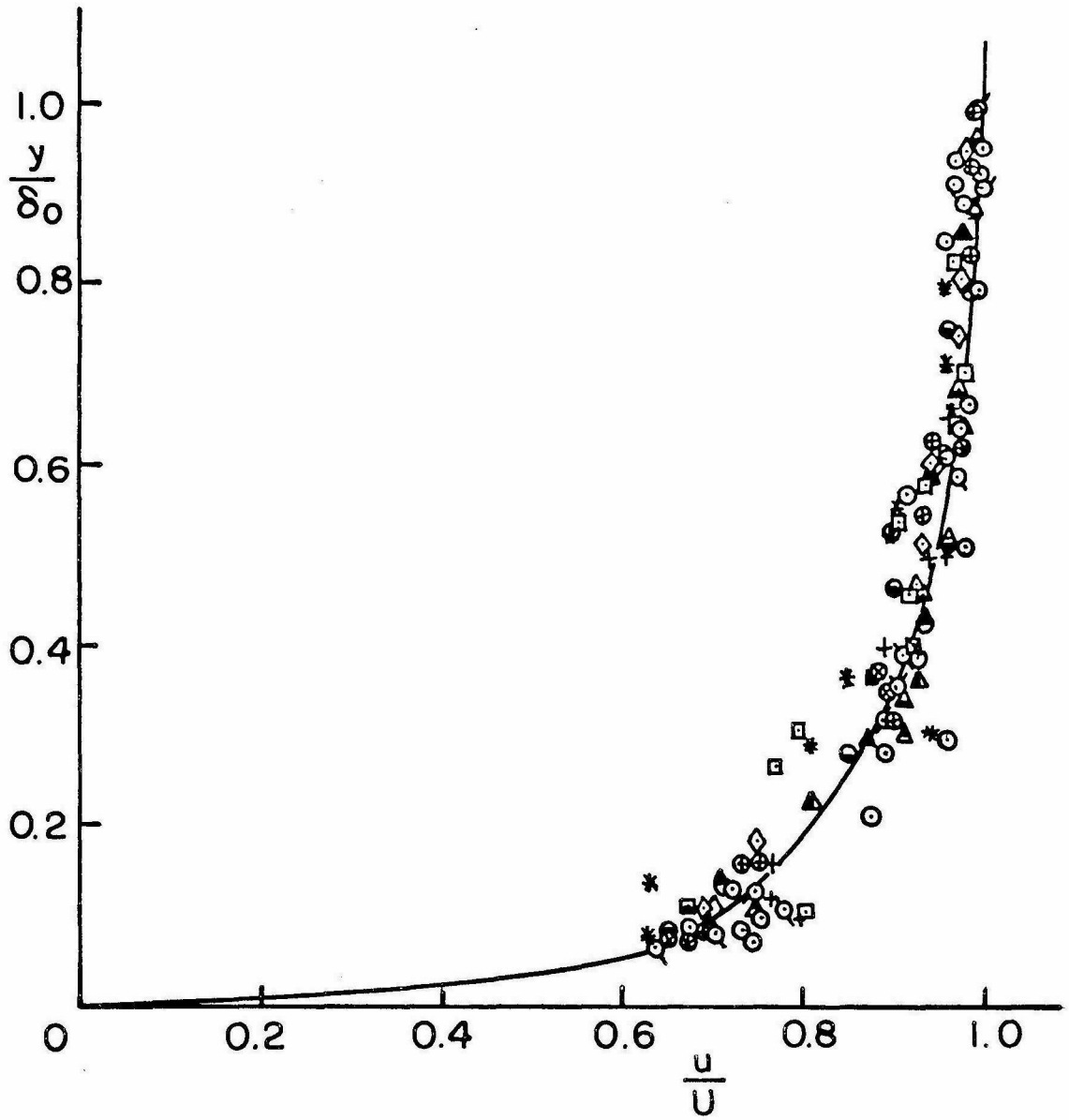

FIG. 10 BOUNDARY LAYER PROFILES AT TWO-DIMENSIONAL JET SLOT EDGE

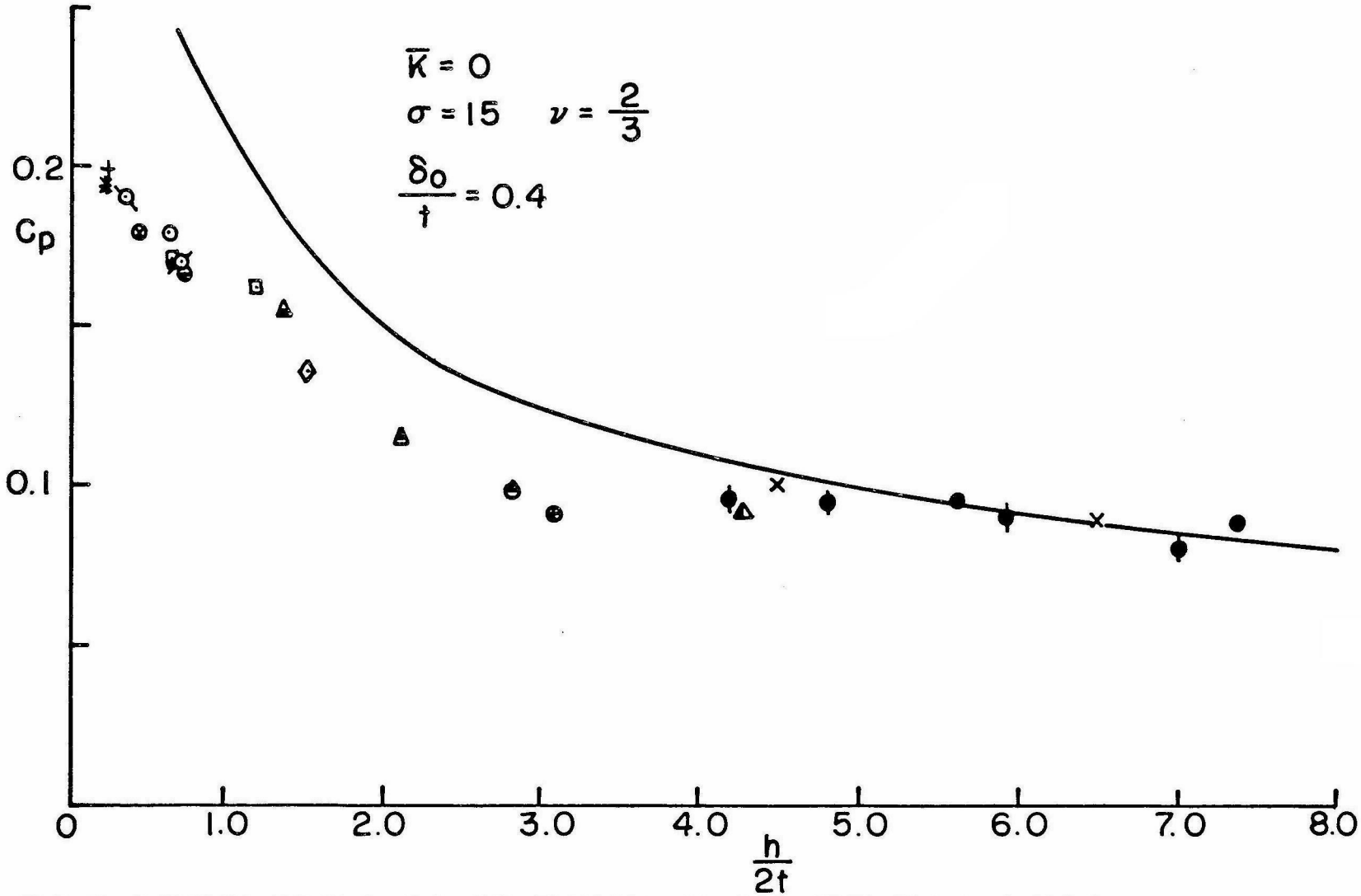

FIG. 11 CAVITY PRESSURE AS FUNCTION OF JET THICKNESS

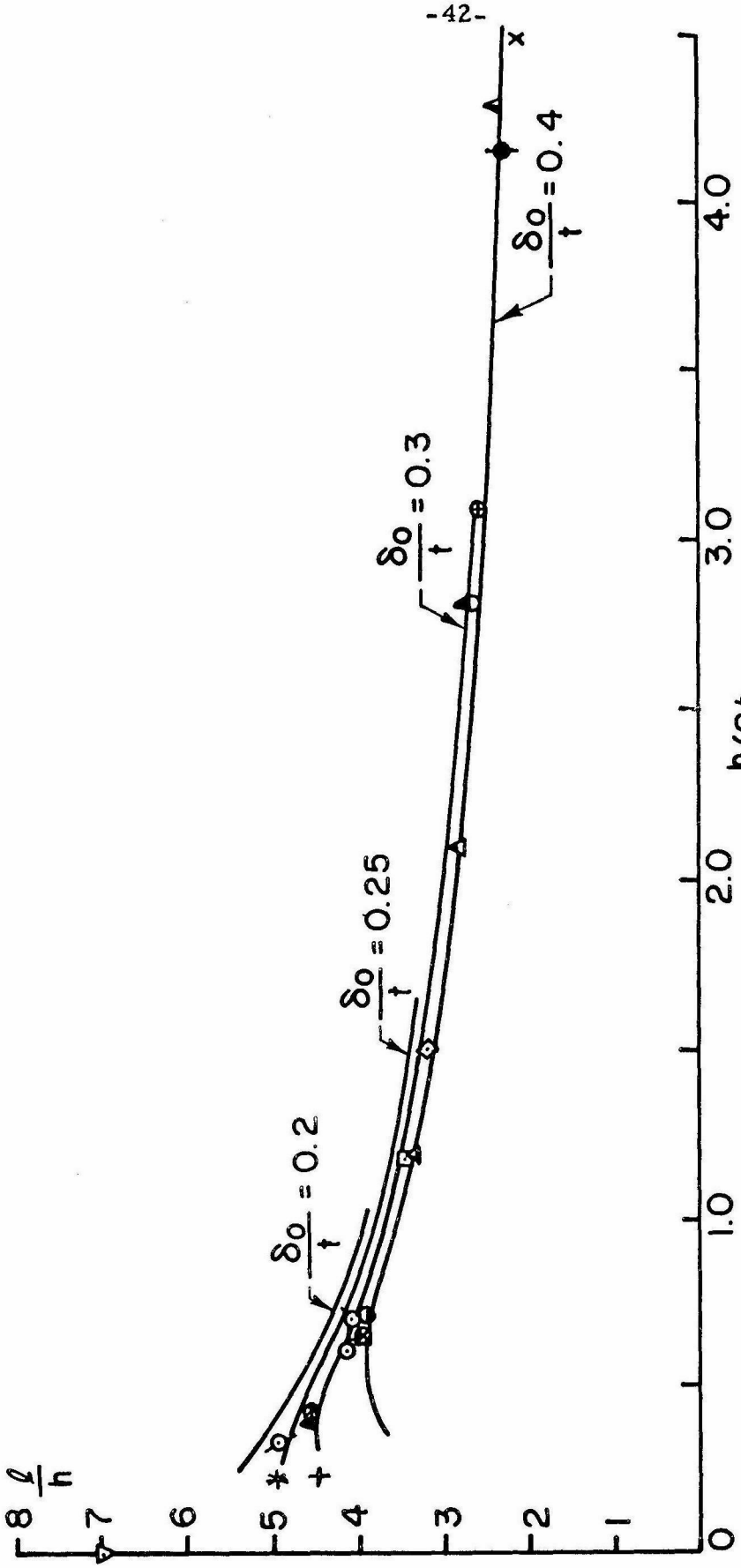

FIG. 12 $\frac{\ell}{h}$ VS $\frac{h}{2t}$ WITHOUT SPANWISE BLOWING, $\overline{K} = \mathcal{K} = 0$, $\sigma = 15$, $\nu = \frac{2}{3}$

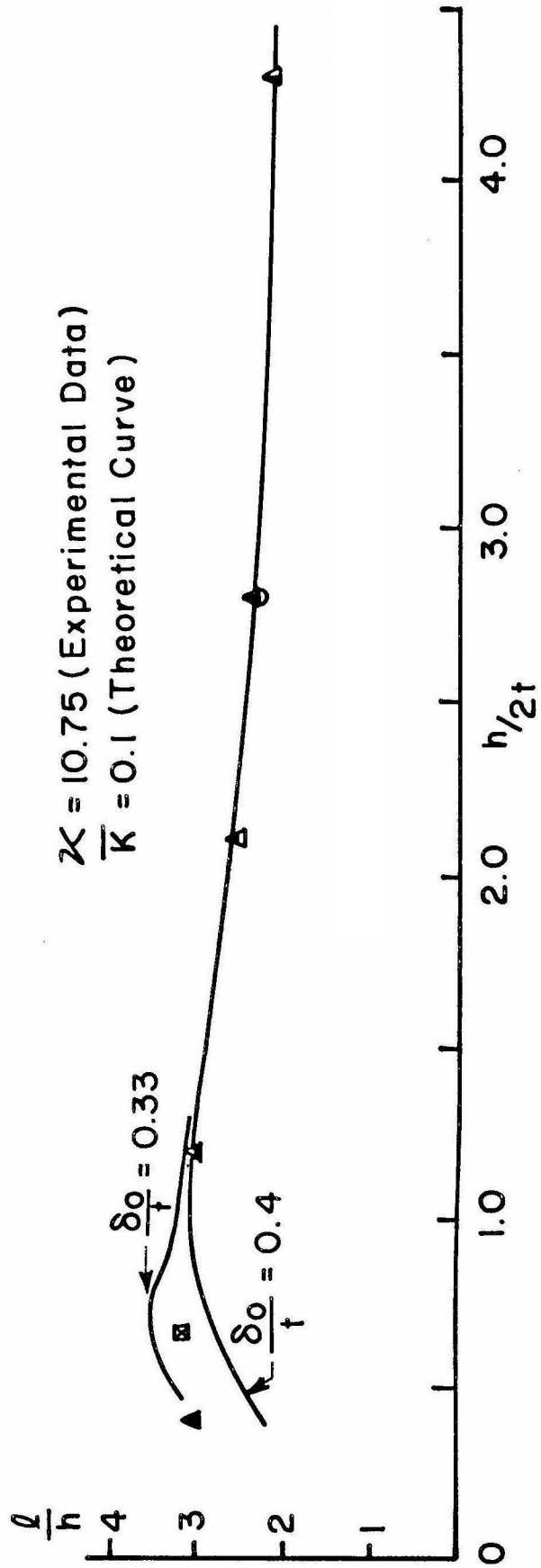

FIG. 13 $\frac{\ell}{h}$ VS $\frac{h}{2t}$ WITH SPANWISE BLOWING, $\overline{K} = 0.1$, $\sigma = 15$, $\nu = \frac{2}{3}$

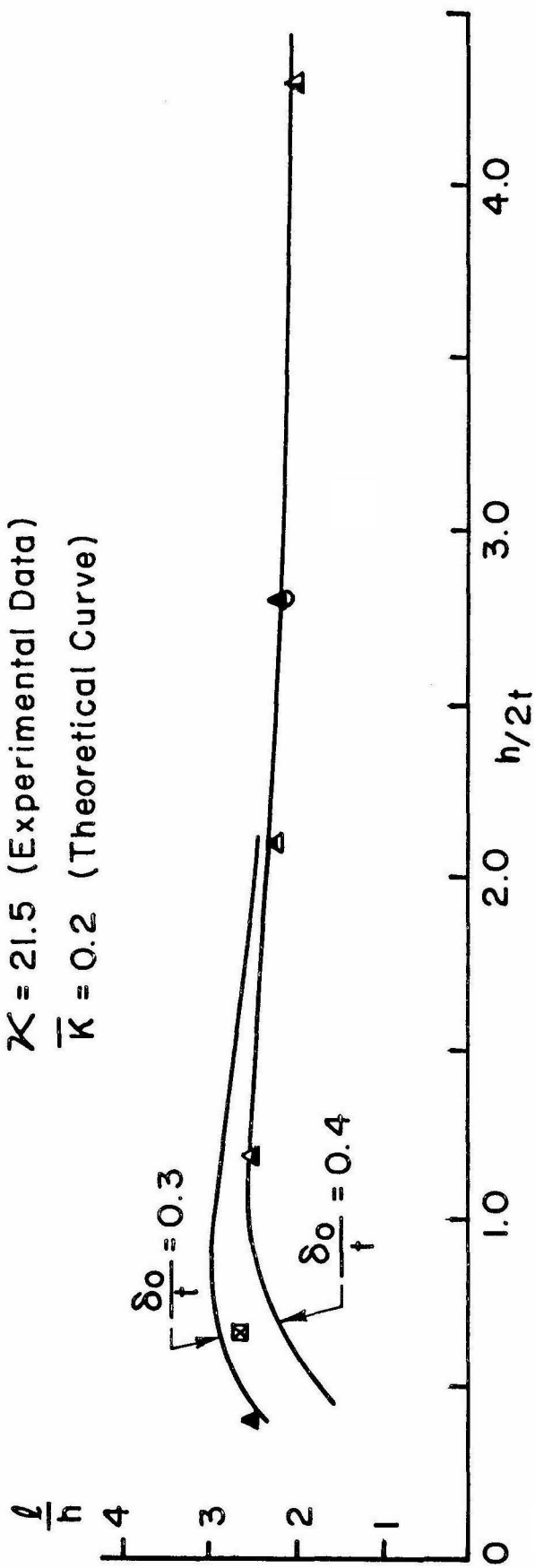

FIG. 14 $\frac{l}{h}$ VS $\frac{h}{2t}$ WITH SPANWISE BLOWING, $\bar{K} = 0.2$, $\sigma = 15$, $\nu = \frac{2}{3}$

Table 1

Without Spanwise Blowing: $\mathcal{K} = 0$

Symbol	h/2t	ℓ/h	C_p	h (in.)	δ_o/t
⊙	0.616	4.19	0.179	3.508	0.246
⊡	1.18	3.44	0.162	4.966	0.228
+	0.246	4.43	0.199	1.036	0.2372
⊕	3.08	2.57	0.091	3.54	0.538
◈	1.504	3.15	0.135	2.826	0.456
⌀	0.70	4.06	0.170	1.898	0.391
⊙	0.339	4.96	0.191	1.170	0.434
✳	0.236	4.96	0.193	1.154	0.348
⊛	0.437	4.55	0.179	1.836	0.328
◒	0.72	3.90	0.167	2.536	0.340
⬓	0.678	4.08	0.172	1.836	0.332
◭	4.30	2.32	0.091	4.820	0.392
◬	2.105	2.81	0.115	4.005	0.484
▲	1.192	3.37	0.154	3.220	0.3848
⊠	0.655	3.99	-	2.340	0.336
▲	0.405	4.58	-	1.700	0.238
⬮	2.82	2.69	0.097	5.367	0.368

Table 1 (Cont'd)

Symbol	h/2t	ℓ/h	C_p	h (in.)	
♦	4.15	2.25	0.096	0.50	Data from Sawyer's Paper (2)
♦	4.81	2.15	0.094		
♦	5.92	2.00	0.089		
♦	6.99	1.97	0.081		
●	5.62	1.96	0.095	1.00	
●	7.35	1.83	0.088		
×	4.5	2.07	0.10		
×	6.5	-	0.095		
×	7.1	1.87	-		
▽	0.00	7.00	-	1.575	From Tani's Paper (6)

With Spanwise Blowing: $\mathcal{K} \neq 0$

Symbol	h/2t	$\mathcal{K} = 10.75$ ℓ/h	$\mathcal{K} = 21.5$ ℓ/h
◭	4.30	2.15	2.00
◭	2.105	2.56	2.27
◭	1.192	3.00	2.54
⊠	0.655	3.15	2.63
▲	0.405	3.00	2.53
⬮	2.82	2.34	2.20